Photophysics

DOI: 10.1002/anie.201101219

Conformational Effects on the Dynamics of Internal Conversion in Boron Dipyrromethene Dyes in Solution**

*Gordon J. Hedley, Arvydas Ruseckas, Anthony Harriman, and Ifor D. W. Samuel**

Electronic energy transfer plays a crucial role in many natural processes, ranging from self-protection[1] to repair mechanisms[2] and energy transduction.[3] One of the primary reasons for employing such indirect excitation is that ideal reagents for inducing chemical change, such as electron transfer or conformational exchange, rarely possess optimal light-absorbing properties.[4] This simple strategy of equipping an elaborate photochemical device with an ancillary photon collector, programmed to absorb over a broad spectral range and to emit at a discrete wavelength, is also relevant to artificial photosynthetic systems. Indeed, such strategies may have relevance to the design of dye-sensitized solar cells[5] and certain organic light-emitting diodes.[6] Similar processes also appear relevant to conducting polymers[7] and solar concentrators.[8] A further, and possibly important, role for light-harvesting units is to promote the harmless dissipation of ultraviolet (UV) photons, arising from increased UVB radiation at the Earth's surface because of stratospheric ozone depletion that would otherwise initiate photo-degradation. The latter realization has led to the recent investigation of cases where an upper-lying excited state (e.g., S_2) of a strongly fluorescent dye functions as the energy acceptor for high-energy photons while the lowest-energy excited state acts as sensitiser for the photonic device.[9] Complementary reports have shown that the S_2 states of certain dyes, notably carotenes[10] and metallo-porphyrins,[11] can be used as energy donors.

In terms of protective mechanisms and device efficacy, it is essential that the S_2 state formed through energy transfer undergoes rapid electronic relaxation (i.e., internal conversion) to the corresponding S_1 state, without opening new routes for deleterious or antagonistic chemical steps. Although the S_2 states of most organic molecules tend to be very short-lived, there are notable exceptions[12] and few rules other than the generic Englman–Jortner energy-gap law[13] by which to predict their lifetimes. Even less is understood about how the internal conversion dynamics depend on the molecular structure and the local environment. We now report on internal conversion in two boron dipyrromethene dyes for which the *meso*-phenyl ring is either constrained (Bodipy) or free to rotate (Robod), the latter class of dye being popular rheology probes.[14] Our particular interest lies with understanding the effect of nuclear motion on the ultrafast dynamics of upper-lying excited states. Earlier work has concluded that deactivation of the higher-lying (i.e., S_3 and/or S_2) excited states and the simultaneous population of the S_1 states of such dyes occur on timescales of a few hundreds of femtoseconds while vibrational cooling of the S_1 state occurs over approximately 20 ps.[15]

The two dyes, Robod and Bodipy (Scheme 1), differ by virtue of the substitution pattern at the pyrrole units. This structural change has an important effect on the photo-

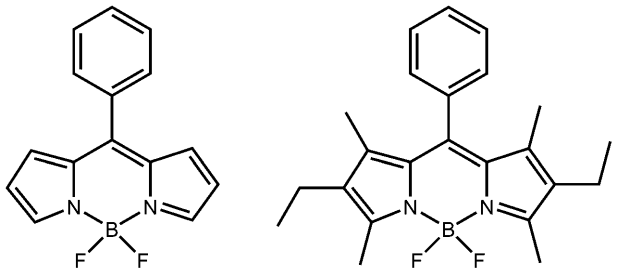

Scheme 1. Molecular structures of the two studied fluorescent dyes. The 4,7-dimethyl groups on the dipyrrin unit hinder rotation of the *meso*-phenyl ring.

physical properties of the S_1 state in that rotation of the phenylene ring distorts the dipyrrin backbone and thereby promotes nonradiative decay of the excited state; this being the origin of the rotor effect.[14] The absorption (ν_{MAX}) and fluorescence (ν_{FLU}) maxima recorded in toluene solution are given in Table 1, together with the measured fluorescence quantum yields (Φ_F) and excited-singlet-state lifetimes (τ_S). Also given are the molar absorption coefficients measured at the peak maximum. The red-shifted absorption and emission spectra in Bodipy are because of the alkyl substituents. The

Table 1: Photophysical properties recorded for the two target dyes in toluene at ambient temperature.

Compound	ν_{MAX} [cm^{-1}]	ε_{MAX} [$M^{-1}cm^{-1}$]	ν_{FLU} [cm^{-1}]	Φ_F	τ_S [ns]
Robod	20080	74500	19305	0.048	0.36
Bodipy	19160	79000	18585	0.69	4.8

[*] Dr. G. J. Hedley, Dr. A. Ruseckas, Prof. I. D. W. Samuel
Organic Semiconductor Centre, SUPA, School of Physics and Astronomy, University of St Andrews
North Haugh, St Andrews, Fife, KY16 9SS (UK)
Fax: (+44) 133-446-3104
E-mail: idws@st-andrews.ac.uk
Prof. A. Harriman
Molecular Photonics Laboratory, School of Chemistry
Bedson Building, Newcastle University
Newcastle upon Tyne, NE1 7RU (UK)

[**] We thank the EPSRC and the Newcastle University for financial support of this work.

Supporting information for this article is available on the WWW under http://dx.doi.org/10.1002/anie.201101219.

much lower fluorescence quantum yield and natural lifetime of Robod indicates a greatly enhanced rate of internal conversion ($S_1 \rightarrow S_0$) because of rapid gyration of the *meso*-phenyl ring in the unhindered dye. While the absorption (and emission) spectral profiles for the S_1 states are sharp and readily resolved into Gaussian components of fairly narrow half-width (i.e., 400 cm^{-1}), the near-UV region shows several overlapping transitions that are considerably weaker and broader than their visible counterparts (see the Supporting Information).

Femtosecond fluorescence up-conversion spectroscopy[16] was used to monitor the rate of internal conversion from the S_2 to S_1 electronic states, with fluorescence from both states being recorded. This approach gives an opportunity to measure the decay time of the S_2 state and the rise-time of S_1 emission, both values embodying the $S_2 \rightarrow S_1$ process. To achieve sufficient absorption in the S_2 region and also to suppress Raman signals from the solvent, concentrated (in the range 1–6 mg mL^{-1}) toluene solutions were employed but no obvious effects on the dynamics were observed over this concentration range. In fact, these dyes are known to be resistant to dimerization in solution.[17] Beginning with 400 nm excitation of Bodipy, emission kinetics accompanying the decay from the S_2 state to S_1 state are shown in Figure 1. Self-absorption by the $S_0 \rightarrow S_1$ transition leads to a smaller recorded signal for direct S_2 emission (the inset shows the kinetics recorded at 450 nm), and hence fitting of these kinetics does not lead to a high degree of precision in the extracted parameters. However, S_1 emission is very strong and thus gives excellent signal to noise, thereby enabling precise fitting of its rise. Emission was detected across the S_1 region and was found to be identical in the 560–600 nm range—with kinetics at 600 nm shown. A rise-time for the signal is very clearly observed; an instantaneous formation (shown as a dot-dash line in Figure 1) plotted for comparison clearly fails to fit the recorded data (this is also shown in the Supporting Information). Instead, the best fit (solid line) gives rise-time constants of 90 fs (97% of the rise amplitude) and 3 ps (3% of the rise amplitude). Both the instantaneous and 90 fs rise-time lines are plotted with respect to the instrument response function (IRF, dotted line), and the correct time zero. Good agreement is found when the same 90 fs and 3 ps parameters are used in the fit of the directly detected S_2 emission at 450 nm (inset, solid line).

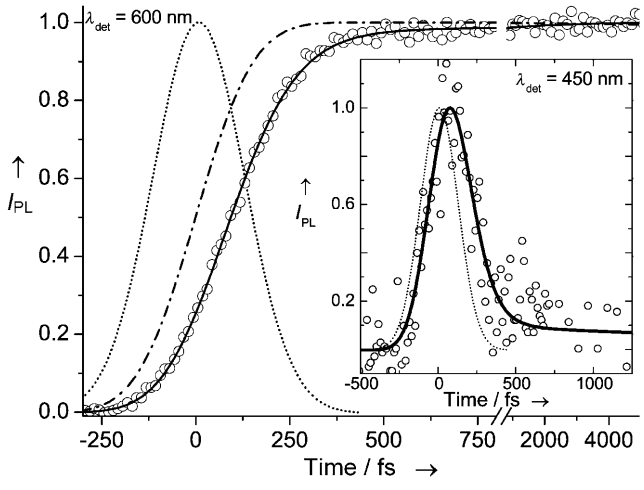

Figure 1. Ultrafast fluorescence kinetics for Bodipy. The main data shows the fluorescence intensity (I_{PL}) as a function of time from the S_1 state detected at 600 nm (λ_{det}) with an excitation wavelength (λ_{ex}) of 400 nm and the instrument response function shown as a dotted line (280 fs FWHM). The dot-dashed line represents the kinetic profile that would exist for an instantaneous formation of the signal. The solid line is the best fit to the data, with a 90 fs rise-time constant constituting 97% of the full amplitude and a 3 ps rise-time constant constituting the remaining 3%. The inset shows emission from the S_2 state detected at 450 nm also with $\lambda_{ex} = 400$ nm, the dotted line indicates the instrument response function (280 fs FWHM) and the solid line is a simulated decay, with time constants of 90 fs (97% of amplitude) and 3 ps (3%) mirroring those found in the rise-time dynamics recorded at 600 nm.

Turning attention now to Robod, both emissions from the S_2 and S_1 states were detected, and the recorded kinetics are shown in Figure 2. Direct detection of internal conversion (i.e., S_2 emission, embodying the $S_2 \rightarrow S_1$ movement) was more difficult than in Bodipy owing to the blue shift in features, leaving less S_2 absorption at the excitation wavelength of 400 nm and more self-absorption from the $S_0 \rightarrow S_1$ transition in the S_2 emission region. Exciting at 380 nm and observing at 425 nm produced detectable emission, but the emission was quite noisy (inset Figure 2), so as with Bodipy, the rise of the S_1 emission was used as a measure of the internal conversion

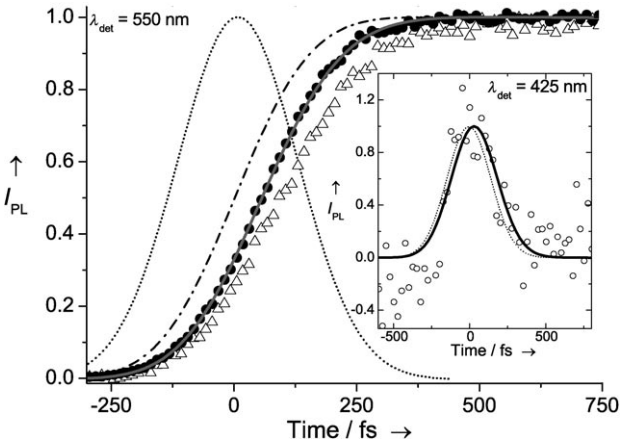

Figure 2. Ultrafast fluorescence kinetics for Robod. The main data (full circles) shows the fluorescence intensity (I_{PL}) as a function of time detected from the S_1 state at 550 nm with $\lambda_{ex} = 400$ nm and the instrument response function displayed as a dotted line (280 fs FWHM). The solid line is the best fit to the data, with a 50 fs rise-time constant constituting 100% of the formation amplitude. The dot-dashed line represents the kinetic profile that would exist for an instantaneous formation of the signal, and the empty triangles show the emission kinetics of the S_1 state of Bodipy from Figure 1, indicating that the emission kinetics of the S_1 state of Robod are clearly different. The inset shows emission from the S_2 state detected at 425 nm with 380 nm excitation, with the dotted line indicating the instrument response function (310 fs FWHM) and the solid line indicating a simulated decay, with a time constant of 50 fs (100% amplitude of the decay), mirroring those found in the rise-time dynamics recorded at 600 nm.

process. The S_1 emission (full circles, Figure 2), obtained by exciting at 400 nm and detecting at 550 nm, gives a best-fit (solid line) rise-time constant of 50 fs (100% of the rise amplitude). An instantaneous (dot-dashed line) rise time is shown for comparison, indicating that is does not fit as well as a 50 fs rise.

Temporally shifted comparisons of rise-time values for Robod are shown in the Supporting Information to indicate that the rise-time of 50 fs fits best. Also plotted in Figure 2 for comparison is the Bodipy S_1 emission data (empty triangles) indicating that there is a clear difference in the formation kinetics between Bodipy and Robod. The best-fit parameters for both dyes thus give different values for the rate of the dominant component of the $S_2 \rightarrow S_1$ internal conversion; namely, 90 fs in Bodipy and 50 fs in Robod. Having established that the two dyes exhibit disparate, but exceedingly fast, rates of internal conversion, attention now turns to the underlying reasons why this is so. The first factor to consider is the $S_2 \rightarrow S_1$ energy gap since this is known to affect the rate of nonradiative deactivation by way of the energy-gap law.[13] The $S_1 \rightarrow S_0$ energy gaps differ by around 800 cm^{-1} (Table 1), according to a Gaussian-band-shape analysis, but, although the spectral profiles differ somewhat in the near-UV region (see Figure S1 in the Supporting Information), the $S_2 \rightarrow S_1$ energy gaps remain constant at around 6100 cm^{-1} for the two dyes. As such, changes in the rate of internal conversion cannot be ascribed to differences in the energy gap between the two states. A further factor to consider, imposed by the structural changes around the dipyrrin framework, relates to the shapes of the potential-energy surfaces (PES) inherent to the excited-state manifolds. Indeed, previous work by Holten and co-workers.[18] on a related dye has explored the effects of the dihedral angle of the phenyl ring with respect to the dipyrrin core, finding that the PES in the dihedral co-ordinate of the S_0 and S_1 states are strongly affected by the presence of methyl groups at the 4,7-positions. These latter groups tend to restrict rotation of the phenyl ring in the case of Bodipy.

Quantum chemical calculations carried out at the PM3/CIDS level for Bodipy indicate that the dihedral angle is around 57° for both S_0 and S_1 states, with the PES being somewhat flattened for the upper-lying state (Figure 3).

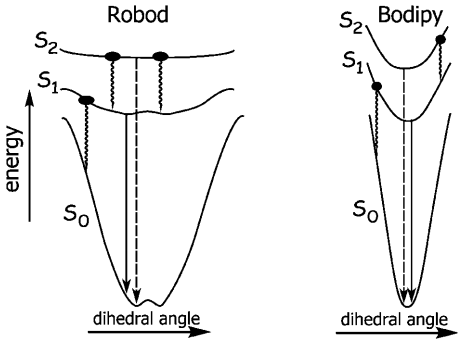

Figure 3. Potential-energy surfaces calculated for the S_0, S_1, and S_2 states of Robod (left-hand side) and Bodipy (right-hand side) with pinhole sinks (black dots) superimposed on the upper surfaces enabling nonradiative internal conversion. Fluorescence from S_1 (solid arrow) and S_2 (dashed arrow) is also shown.

Further PES flattening is to be expected for the S_2 state, because of the increased energy content, although the computations become less precise as we move up the electronic ladder. Such generic behavior is fully consistent with the fact that the photophysical properties of Bodipy are independent of temperature and solvent viscosity. This is not the case for Robod, where full rotation of the phenyl ring is hindered but possible while the S_1 PES shows a shallow barrier to rotation (Figure 3). The initially prepared excited-state population diffuses along the PES by a random walk, searching for regions where the surface is more strongly coupled to the S_0 PES. The upward curvature of the PES presents a barrier for such one-dimensional diffusion. To account for the rotor effect observed with Robod, but not Bodipy, it has been proposed[14] that the S_1 PES for Robod contains areas which are close in energy to the S_0 PES, denoted as local pinhole sinks, that are strongly coupled to the S_0 surface,[19] enabling fast nonradiative relaxation. These pinholes, which funnel the excited-state population down to the ground state, are situated on the PES in such a way that frictional forces with surrounding solvent molecules affect the frequency with which they are accessed. For both dyes, radiative decay of the S_1 state occurs from the relaxed geometry.

This description can be applied to the S_2 states so as to account for the rapid rate of internal conversion (Figure 3). For Bodipy, the S_2 PES is considered to be relatively shallow, but not flat, and containing nonlocal pinhole sinks that facilitate rapid internal conversion. This situation would give rise to fast, dual-exponential kinetics; the decay rate being set by the time needed to diffuse along the PES to one of the holes.[20] The bulky methyl groups impose some curvature on the PES, which appears in the form of a barrier to reaching any surface holes that might funnel the wave-packet down to the S_1 state. For Robod, the S_2 PES is considered to be almost flat such that there is no real barrier to reaching the pinhole sinks. In this case, decay of the S_2 state will be mono-exponential and very fast. The rate at which the wave-packet passes through the funnel will be exponentially dependent on the energy gap between the S_2 and S_1 PESs at that particular nuclear geometry. It is interesting to note that while the rate of $S_2 \rightarrow S_1$ internal conversion is different for Robod and Bodipy, the relative change in the rate is much smaller than the $S_1 \rightarrow S_0$ relaxation, though the latter can be related to the energy gap between the states.

To summarize, we have noted that the molecular structure influences the rate of internal conversion between the S_2 and S_1 excited states in two fluorescent dyes of great topical interest. The key structural facet relates to gyration of the *meso*-phenyl ring as controlled by the secondary substituents. These results represent the first direct illustration of how the dynamics of internal conversion between S_2 and S_1 excited states can be modulated by minor variations of the molecular backbone. The importance of low-frequency vibronic modes in promoting fast internal conversion should be stressed. It has already been established that these S_2 states operate as highly effective acceptors for UV photons and that the dyes are highly attractive solar concentrators.[8] In this way, such dyes could have important applications to help intricate

photonic devices overcome the negative impact of exposure to increased levels of UV radiation.

Experimental Section

Samples of the Bodipy dyes were synthesized and purified by conventional methods. Quantum chemical calculations were performed with AMPAC. Ultrafast luminescence measurements were performed with upconversion spectroscopy[16] using the FOG100 by CDP systems as reported previously.[21] The instrument response function was measured by recording the Raman signal generated by a sample cell containing water, and was found to be 280 fs (full width at half maximum, FWHM) at 400 nm excitation and 310 fs at 380 nm.

Received: February 17, 2011
Revised: May 9, 2011
Published online: June 10, 2011

Keywords: emission spectroscopy · kinetics · laser chemistry · photophysics · time-resolved spectroscopy

[1] a) H. Lee, Y. C. Cheng, G. R. Fleming, *Science* **2007**, *316*, 1462 – 1465; b) B. Loll, J. Kern, W. Saenger, A. Zouni, J. Biesiadka, *Nature* **2005**, *438*, 1040 – 1044.

[2] a) G. Cerullo, D. Poll, G. Lanzani, S. De Silvestri, H. Hashimoto, R. J. Cogdell, *Science* **2002**, *298*, 2395 – 2398; b) A. C. Benniston, A. Harriman, *Mater. Today* **2008**, *11*, 26 – 34; c) J. F. Allen, J. A. Raven, *J. Mol. Evol.* **1996**, *42*, 482 – 492.

[3] a) S. Eberhard, G. Finazzi, F. A. Wollman, *Annu. Rev. Genet.* **2008**, *42*, 463 – 515; b) P. E. Jensen, R. Bassi, E. J. Boekema, J. P. Dekkar, S. Jansson, D. Leister, C. Robinson, H. V. Schellar, *Biochim. Biophys. Acta Bioenerg.* **2007**, *1767*, 335 – 352; c) D. Gust, T. A. Moore, A. L. Moore, *Acc. Chem. Res.* **2001**, *34*, 40 – 48.

[4] a) G. D. Scholes, G. R. Fleming, *Adv. Chem. Phys.* **2006**, *132*, 57 – 71; b) M. Fujihashi, N. Numoto, Y. Kobayashi, A. Mizushima, M. Tsujimura, A. Nakamura, Y. Kawarabayashi, *J. Mol. Biol.* **2007**, *365*, 903 – 910; c) C. Saxena, A. Sancar, D. P. Zhong, *J. Phys. Chem. B* **2004**, *108*, 18026 – 18033.

[5] S. Hayashi, M. Tanaka, H. Hayashi, S. Eu, T. Umeyama, Y. Matano, Y. Araki, H. Imarhori, *J. Phys. Chem. C* **2008**, *112*, 15576 – 15585.

[6] V. A. Montes, C. Perez-Bolivar, N. Agarwal, J. Shinar, P. Anzenbacher, *J. Am. Chem. Soc.* **2006**, *128*, 12436 – 12438.

[7] J. Singh, E. R. Bittner, D. Beljonne, G. D. Scholes, *J. Chem. Phys.* **2009**, *131*, 194905.

[8] A. Harriman, L. J. Mallon, K. J. Elliott, A. Haefele, G. Ulrich, R. Ziessel, *J. Am. Chem. Soc.* **2009**, *131*, 13375 – 13386.

[9] A. Harriman, L. J. Mallon, S. Goeb, G. Ulrich, R. Ziessel, *Chem. Eur. J.* **2009**, *15*, 4553 – 4564.

[10] a) A. N. MacPherson, J. B. Arellano, N. J. Fraser, R. J. Cogdell, T. Gillbro, *Biophys. J.* **2001**, *80*, 923 – 930; b) S. Akimoto, S. Takaichi, T. Ogata, Y. Nishimura, I. Yamazaki, M. Mimuro, *Chem. Phys. Lett.* **1996**, *260*, 147 – 152; c) H. Cong, D. M. Niedzwiedzki, G. N. Gibson, A. M. LaFountain, R. M. Kelsh, A. T. Gardiner, R. J. Cogdell, H. A. Frank, *J. Phys. Chem. B* **2008**, *112*, 10689 – 10703; d) H. A. Frank, R. Farhoosh, M. L. Aldema, B. DeCoster, R. L. Christensen, R. Gebhard, J. Lugtenburg, *Photochem. Photobiol.* **1993**, *57*, 49 – 55; e) M. P. Debreczeny, M. R. Wasielewski, S. Shinoda, A. Osuka, *J. Am. Chem. Soc.* **1997**, *119*, 6407 – 6414.

[11] A. Harriman, M. Hissler, O. Trompette, R. Ziessel, *J. Am. Chem. Soc.* **1999**, *121*, 2516 – 2525.

[12] a) E. K. L. Yeow, R. P. Steer, *Phys. Chem. Chem. Phys.* **2003**, *5*, 97 – 105; b) W. Adam, W. J. Baader, L. H. Catalani, G. Cilento, L. Rychla, *Photochem. Photobiol.* **1985**, *42*, 587 – 589.

[13] R. Englman, J. Jortner, *Mol. Phys.* **1970**, *18*, 145 – 164.

[14] M. A. H. Alamiry, A. C. Benniston, G. Copley, K. J. Elliott, A. Harriman, B. Stewart, Y.-G. Zhi, *Chem. Mater.* **2008**, *20*, 4024 – 4032.

[15] P. Toele, H. Zhang, C. Trieflinger, J. Daub, M. Glasbeek, *Chem. Phys. Lett.* **2003**, *368*, 66 – 75.

[16] J. Shah, *IEEE J. Quantum Electron.* **1988**, *24*, 276 – 280.

[17] G. Ulrich, R. Ziessel, A. Harriman, *Angew. Chem.* **2008**, *120*, 1202 – 1219; *Angew. Chem. Int. Ed.* **2008**, *47*, 1184 – 1201.

[18] H. L. Kee, C. Kirmaier, L. Yu, P. Thamyongkit, W. J. Youngblood, M. E. Calder, L. Ramos, B. C. Noll, D. F. Bocian, W. R. Scheidt, R. R. Birge, J. S. Lindsey, D. Holten, *J. Phys. Chem. B* **2005**, *109*, 20433 – 20443.

[19] D. Ben-Amotz, C. B. Harris, *J. Chem. Phys.* **1987**, *86*, 4856 – 4870.

[20] a) G. Oster, Y. Nishijima, *J. Am. Chem. Soc.* **1956**, *78*, 1581 – 1584; b) T. Förster, G. Hoffmann, *Z. Phys. Chem. NF* **1971**, *75*, 63 – 76; c) B. Bagchi, G. R. Fleming, D. W. Oxtoby, *J. Chem. Phys.* **1983**, *78*, 7375 – 7384.

[21] G. J. Hedley, A. Ruseckas, I. D. W. Samuel, *J. Phys. Chem. A* **2010**, *114*, 8961 – 8968.

